Biomechanical Comparison of Different Surface Modifications for Dental Implants

Stephen J. Ferguson, PhD[1]/Jens D. Langhoff, Dr Med Vet[2]/Katrin Voelter, Dr Med Vet[2]/
Brigitte von Rechenberg, Dr Med Vet, PhD[3]/Dieter Scharnweber, PhD[4]/Susanne Bierbaum, PhD[5]/
Matthias Schnabelrauch, PhD[6]/Armin R. Kautz, PhD[7]/Vinzenz M. Frauchiger, PhD[8]/
Thomas L. Mueller, MSc[9]/G. Harry van Lenthe, PhD[10]/Falko Schlottig, PhD[11]

Purpose: A satisfactory clinical outcome in dental implant treatment relies on primary stability for immediate load bearing. While the geometric design of an implant contributes to mechanical stability, the nature of the implant surface itself is also critically important. Biomechanical and microcomputerized tomographic evaluation of implant osseointegration was performed to compare alternative structural, chemical and biochemical, and/or pharmaceutical surface treatments applied to an identical established implant design. *Materials and Methods:* Dental implants with the same geometry but with 6 different surface treatments were tested in vivo in a sheep model (pelvis). Peri-implant bone density and removal torque were compared at 2, 4, and 8 weeks after implantation. Implant surfaces tested were: sandblasted and acid-etched titanium (Ti), sandblasted and etched zirconia, Ti coated with calcium phosphate (CaP), Ti modified via anodic plasma-chemical treatment (APC), bisphosphonate-coated Ti (Ti + Bisphos), and Ti coated with collagen containing chondroitin sulfate (CS). *Results:* All dental implants were well integrated at the time of sacrifice. There were no significant differences observed in peri-implant bone density between implant groups. After 8 weeks of healing, removal torque values for Ti, Ti + CaP, Ti + Bisphos, and Ti + collagen + CS were significantly higher than those for zirconia and Ti + APC. *Conclusions:* Whereas the sandblasted/acid-etched Ti implant can still be considered the reference standard surface for dental implants, functional surface modifications such as bisphosphonate or collagen coating seem to enhance early peri-implant bone formation and should be studied further. INT J ORAL MAXILLOFAC IMPLANTS 2008;23:1037–1046

Key words: *biomechanics, bisphosphonate, collagen, dental implant, osseointegration*

[1]Reseach Division Head, Institute for Surgical Technology and Biomechanics, University of Bern, Switzerland.
[2]Researcher, Musculoskeletal Research Unit, University of Zürich, Switzerland.
[3]Professor, Musculoskeletal Research Unit, University of Zürich, Switzerland.
[4]Head of Biomaterials Development, Max Bergmann Center for Biomaterials, Institute of Materials Science, Dresden University of Technology, Dresden, Germany.
[5]Project Manager R & D, Max Bergmann Center for Biomaterials, Institute of Materials Science, Dresden University of Technology, Dresden, Germany.
[6]Head of Biomaterials Research, Biomaterials Department, Innovent, Jena, Germany.
[7]Researcher, Biomaterials Department, Innovent, Jena, Germany.
[8]Researcher, Dr Robert Mathys Foundation, Bettlach, Switzerland.
[9]Researcher, Institute for Biomechanics, Eldgenossische Technische Hochschule Zürich, Zürich, Switzerland.
[10]Associate Professor, Institute for Biomechanics, Eldgenossische Technische Hochschule Zürich, Zürich, Switzerland.
[11]Head of Research, Thommen Medical, Waldenburg, Switzerland

Correspondence to: PD Dr Stephen Ferguson, University of Bern, Institute for Surgical Technology and Biomechanics, Stauffacherstrasse 78, CH-3014 Bern, Switzerland. E-mail: stephen.ferguson@artorg.unibe.ch

The use of osseointegrated dental implants is recognized as a predictable and successful treatment method for functional restoration of the fully or partially edentulous patient. A satisfactory clinical outcome relies on the ability of the implant to bear loads, which is a function of the primary stability immediately following implantation but is dependent on solid osseointegration of the implant into the host bone for the long term. The nature of the implant surface itself is of critical importance for the progression toward osseointegration.[1] The most important surface properties are topography, chemistry, surface charge, and wettability. Processes such as protein adsorption, cell-surface interaction, and cell/tissue development at the interface between the implant and host bone are affected by implant surface properties[2] and are all relevant for the function of the device.

In the past, substantial efforts have been made to optimize the topography of dental implant surfaces to accelerate the healing process. Titanium surfaces with microscopic scale roughness have been proposed as an alternative to more conventional implant surfaces produced by machining or titanium

plasma spraying. Microrough titanium surfaces have been produced using various techniques, including sandblasting, acid etching, and combinations of both, to create a modified surface topography.[3] The sandblasted and acid-etched surface has demonstrated enhanced bone apposition in histomorphometric studies[4,5] and higher removal torque values in biomechanical testing,[6,7] indicating a direct relationship between the biologic and mechanical quality of the interface, as well as excellent mid- to long-term clinical results.[8–11]

Less is known about the combined effect of surface topography and chemistry, an important synergistic potential for optimizing healing time. Chemical and biochemical surface modifications are assumed to be especially advantageous for accelerated healing. A modified sandblasted/acid-etched surface has been shown to enhance surface wettability and also improve osseointegration and interfacial strength.[12] The potential of a new generation of thin calcium phosphate (CaP) –based coatings has been described by several authors.[13,14] Fluoride surface modification seems to enhance osteoblastic differentiation and interfacial bone formation.[15] Another approach is a functionalized poly(L-lysine) and poly(ethylene glycol) copolymer (PLL-g-PEG) coating, which inhibits in vitro bacterial growth and interacts with osteoblasts through the integrated bioligands.[16] The modification of biochemistry using biologically altered surfaces has been shown. The use of modified titanium surfaces with extracellular matrix components enhances bone remodeling in the early stages of healing; a significant increase in osteopontin-positive osteoblasts was observed next to arginine-glycine-aspartic acid (RGD) peptide–coated implants.[17] A newer approach is surface modification with bioactive molecules. Nucleic acid single strands are fixed electrochemically via their termini (regiospecifically) by anodically growing an oxide layer on titanium-aluminum-niobium (Ti-6Al-7Nb).[18] Drug-eluting coatings are the most probable future developments. Local delivery of bisphosphonates has resulted in increases in the mechanical fixation of implants,[19] while the potential of growth factors such as bone morphogenetic protein 2 has been shown in many studies.[20,21]

Clearly, there are many potential candidates for the "optimal" surface of dental implants, along with a lack of comparative data. Therefore, the purpose of this study was to perform biomechanical and microcomputerized tomographic (microCT) evaluation of implant osseointegration to compare alternative structural, chemical and biochemical, and/or pharmaceutical surface treatments using a well-established implant design.

MATERIALS AND METHODS

Implant Design

Six different implant surface types were evaluated: 5 surface-modified, commercially pure titanium implants and 1 surface-modified zirconia implant were employed. Eighteen implants were used in each group. Implant shape was identical to the standard SPI Implant configuration, with a 4.2-mm diameter and 8-mm length (Thommen Medical, Waldenburg, Switzerland). Implant surface types were as follows.

- *Group 1:* Titanium implants were sandblasted and acid etched.
- *Group 2:* Zirconia implants (yttrium partially stabilized zirconia, medical grade) were sandblasted and etched in an alkaline bath.
- *Group 3:* CaP was coated via electrochemical assistance onto sandblasted and acid-etched titanium implants. The implants were coated in an aqueous solution containing Ca and phosphate ions. The coating consists of the 2 CaP phases hydroxyapatite and brushite and is commercially available.[22]
- *Group 4:* The implants were treated with the anodic plasma-chemical surface modification method (APC) after sandblasting. APC is an advanced anodization method that allows for anodic oxide layer formation and incorporation of CaP phases in a single step. The method exploits the dielectric breakdown of anodic oxide films to produce a porous oxide layer that contains significant amounts of electrolyte components. The electrolyte contained calcium and phosphate ions, leading to a CaP-containing porous surface.[23]
- *Group 5:* The implants were coated with bisphosphonate. Sandblasted and acid-etched titanium implants were spray coated with a suspension to a final alendronate concentration of 10 µg/cm^2. The suspension was prepared by treating an alendronate sodium salt with sodium dodecyl sulfate, resulting in a sparingly soluble salt.
- *Group 6:* Sandblasted and acid-etched implants were coated with an artificial extracellular matrix from acid-soluble bovine collagen type I and chondroitin sulfate (CS). To create the latter, CS at a concentration of 30 µg/mg collagen was added on ice to a fibrillogenesis buffer solution containing 2.5 mg/mL collagen. Fibrillogenesis was allowed to take place overnight at 37°C. The resulting gel was homogenized and fibrils were collected by centrifugation, washed with fibrillogenesis buffer, and centrifuged again. The pellet was resuspended in the same buffer to a concentration of about 5 mg/mL collagen. The implants were incubated in the suspension at 25°C for 5 min and air

dried. This process was performed a total of 2 times. The coated implants were then washed with distilled water and sterilized.[24]

Surface Topography

Roughness measurements were performed using a confocal microscope (Nanofocus μsurf, Oberhausen, Germany) over an area of 320 × 308 μm (lateral resolution 0.7 μm, vertical resolution 25 nm). The roughness values were calculated after the subtraction of the third-order area regression taking the whole area into account (not only profiles). All roughness values were calculated using the WinSAM 2.6 software package (Lehrstuhl für Fertigungstechnologie, Universität Erlangen, Nuremberg, Germany). For electron microscopy, a Cambridge S360 instrument (Carl Zeiss NTS, Oberkochen, Germany) was used. Secondary electron images were recorded using an acceleration voltage of 20 kV and a sample current of 200 pA.

Study Design and Animal Model

The animal experiment was conducted according to Swiss law for animal protection and welfare, and permission was obtained from the local authorities (State of Zurich, permission no. 159/2005). A previously developed sheep model served as an accepted model for human bone healing and osseointegration.[25,26] All implants were placed in the iliac bone of the pelvis, with 7 implants per side (one implant type was not evaluated for the present study). The iliac crest offers a broad variety of bone qualities, ranging from almost purely cancellous (less than 0.5 mm cortical thickness) to compact cortical bone (up to 3 mm in thickness). Regarding bone quality, this allows comparison to the bone found in the mandible as classified in the Lekholm and Zarb index.[27] The study examined 3 essential phases of implant osseointegration: the acute phase (2 weeks), the early phase (4 weeks), and the continued phase (8 weeks), with 5 animals per time point. An implantation scheme was designed to achieve a homogeneous spatial distribution of all implant types, with a sample size of 6 per implant group and healing time for biomechanical testing (total n = 108) (Fig 1). Additional implants were placed for a concurrent histomorphometric analysis, the topic of a separate study.

Surgical Procedure

The access to each iliac crest was gained from the dorsolateral by a standard surgical procedure. Equally spaced cavities for the dental implants were prepared using a 2.0-mm pilot drill, then expanded with 2.8-mm and 3.5-mm drills (SPI VECTOdrill, Thommen Medical, Waldenburg, Switzerland). A specially constructed drill sleeve was used to ensure a standardized drill depth, which was confirmed with a depth

Fig 1 Dorsal view of sheep pelvis, with implantation sites indicated. A total of 108 implants was placed for the biomechanical study (6 groups × 6 implants × 3 healing periods).

gauge. Self-tapping implants (SPI ELEMENT, Thommen Medical) were placed according to a randomized implantation scheme (randomized location of the 6 implant types). Implants were covered with a healing cap and tightened with a torque wrench. After completion, the muscle was repositioned and the tendinous insertion was resutured to its origin. The fascia and subcutis were closed using synthetic resorbable sutures and the skin was closed with staples.

Sample Collection

Animals were euthanized following the predefined healing periods. The implantation sites were harvested with the full pelvic bone within 10 minutes postmortem. The iliac bone was sectioned with an oscillating saw into individual bone blocks, each of which contained 1 implant with at least 12 mm of adjacent bone tissue. Bone blocks for mechanical testing were wrapped in gauze soaked with an isotonic sodium chloride solution and tightly packed in plastic bags to prevent drying. Samples were stored at 7°C until testing (maximum 36 hours).

Removal Torque Testing

The removal torque testing protocol has been previously described in detail.[6] To facilitate specimen handling and to provide adequate temperature isolation, each bone block was embedded in fast-curing dental cement (GC Fujirock, GC Europe, Leuven, Belgium). Removal torque testing was performed on a servohydraulic biaxial testing machine (MTS MiniBionix 358; MTS, Minneapolis, MN, USA). The implant was first attached to the upper hydraulic actuator via a custom-machined adapter, thus guaranteeing alignment of the implant with the actuator's rotational axis. The adapter for coupling the implant to the hydraulic actuator was vertically unconstrained to

Fig 2 Three-dimensional segmented microCT images. The implant is marked in red, whereas bone is shown in grey. The 2 trabecular volumes of interest are shown in orange (outer ring, "nonaffected bone") and yellow (inner ring).
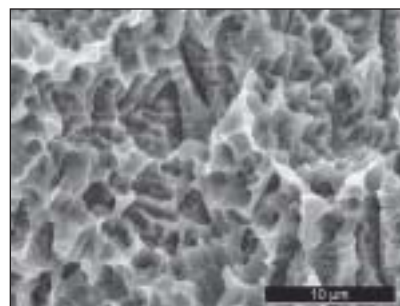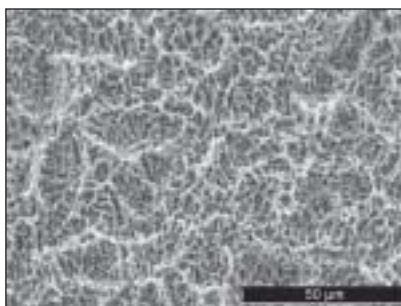
Figs 3a and 3b Scanning electron micrographs of group 1 surface (sandblasted and acid-etched titanium implant).

eliminate any axial load on the implant. The implant-bone-cement specimen was then lowered into a metal container, and the space surrounding the specimen was filled with a low-melting-temperature metal alloy (Ostalloy 117, Legierung 47° Grad FA16; Metallum, Pratteln, Switzerland). Solidification of the alloy proceeded quickly, minimizing specimen heating and achieving rigid fixation of the specimen in the machine. Removal torque testing was performed by rotating the implant counterclockwise at a rate of 0.1 degree per second to a maximum angle of 30 degrees while simultaneously collecting angle and torque data at a sampling rate of 10 Hz. The specimens were kept moist throughout testing by spraying with saline solution, and the bone temperature was maintained at 29°C ± 0.5°C throughout.

The resulting torque-rotation curve was analyzed to determine the removal torque value and failure mode. The removal torque (N-mm) was defined as the maximum torque recorded on the curve for specimens that showed a clear peak and subsequent drop in torque. For specimens with a constantly increasing torque-rotation curve, or a plateau in the measured torque values, a yield point was defined by constructing a straight line parallel to the initial slope of the torque-rotation curve, offsetting this by 0.72 degrees (0.2% full rotation), and then selecting the intersection of this offset line with the original torque-rotation curve.

MicroCT

For nondestructive 3-dimensional characterization of peri-implant bone, selected samples were subsequently scanned and analyzed by microCT.[28] One hundred samples were measured (fifty 4-week samples and fifty 8-week samples) using a commercial imaging device (μCT40, Scanco Medical, Bassersdorf, Switzerland) and applying an isotropic resolution of 30 μm. The analyzed sections comprised an evenly distributed sample from both the biomechanical testing and the concurrent histomorphometry study. Two global threshold levels were applied to the filtered

data to distinguish between implant, mineralized tissue, and background. Special image processing[29] was applied to the direct vicinity of the implant to remove imaging artifacts. For quantitative analysis, 2 cylindric volumes of interest (VOIs) were defined (Fig 2). The first VOI had a diameter of 6 mm centered around the implant (the "inner ring"); the second VOI was a hollow cylinder with inner and outer radii of 10 and 12 mm, respectively (the "outer ring"; Fig 2). Each volume was analyzed for bone volume density (ie, bone volume/total volume [BV/TV]). MicroCT is a precise and validated technique that provides accurate measures of bone volume and architecture.[30]

Statistical Analysis

The removal torque (dependent variable) was analyzed, using a factorial analysis of variance (ANOVA) with interactions, for the effect of the following independent factors: implant surface type, implant position, and healing period. Post hoc comparisons were made using the Scheffé F test. All analyses were performed using the ANOVA/MANOVA module of Statistica 7.0 (StatSoft, Tulsa, OK). The correlation between local bone density and removal torque values was evaluated using linear regression analysis. A significance level of $P = .05$ was defined.

RESULTS

Characterization of Surfaces

Figure 3 shows a typical sandblasted and acid-etched surface (group 1). The micropits produced by the etching process are shown in Fig 3a, and the macrorough surface texture caused by the sandblasting process can clearly be seen in Fig 3b. The sandblasted and etched zirconia surface (group 2) shows a completely different topography. The microroughness appears cauliflowerlike (Fig 4a), and the macroroughness is less pronounced (Fig 4b). Figures 5a and 5b show the typical structural elements of the electrochemically deposited coating (group 3).

Figs 4a and 4b   Scanning electron micrographs of group 2 surface (sandblasted and alkaline-etched zirconia implant).
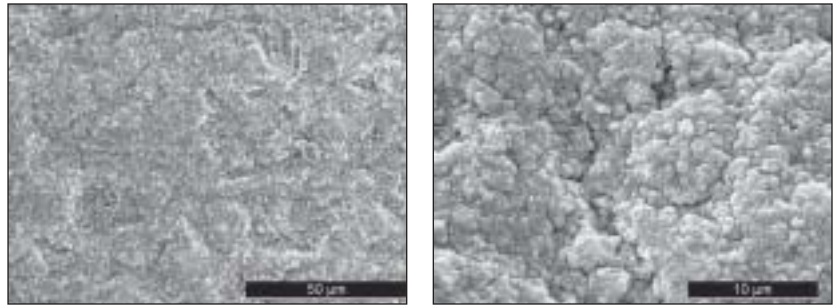
Figs 5a and 5b   Scanning electron micrographs of group 3 surface (sandblasted and acid-etched titanium implant with surface electrochemically coated with calcium phosphate).
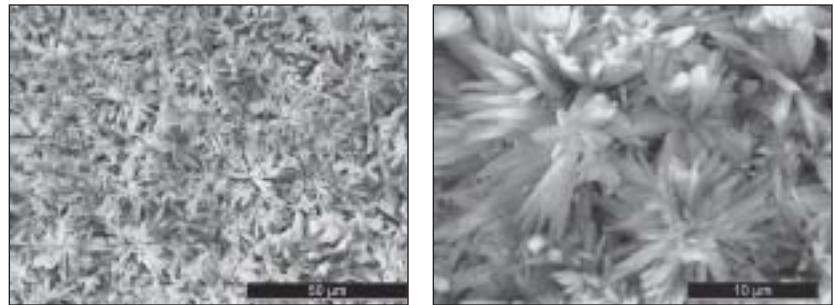
Figs 6a and 6b   Scanning electron micrographs of group 4 surface (sandblasted titanium implant treated with the anodic plasma-chemical surface modification method).
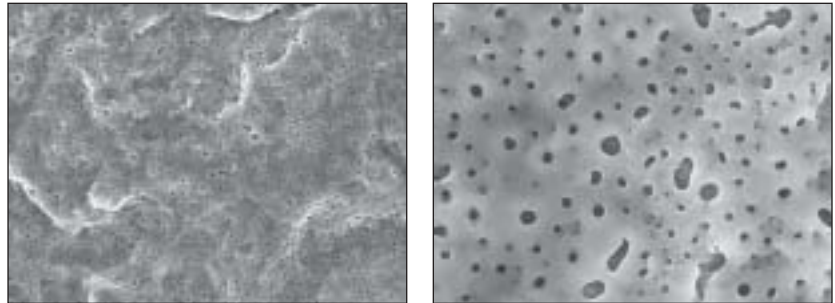
The figures show clearly the fine crystalline coating structure with fixed CaP crystallites in the shape of platelets or pins. The APC-modified surface structure is shown in Fig 6 (group 4). The surface layer is porous and composed of small craters with holes in the center. In contrast, the bisphosphonate-coated implants (group 5, Fig 7) show no difference from the uncoated group 1 implants under the selected imaging conditions. A different pattern for the collagen containing CS–coated (CCCS) (group 6) implants is apparent (Fig 8). The topographic properties of the investigated implant surfaces are shown in Table 1.

MicroCT

Bone volume density (BV/TV) at the outer ring was similar for all implant types, and no significant changes were found between the 4-week and the 8-week samples. BV/TV at the inner ring was between 40% and 63% higher than at the outer ring. This difference in BV/TV was significant for all implant

groups as well as for both time points (Table 2). Time-dependent changes in BV/TV did not reach significance for any of the implants.

Biomechanical Testing

Representative examples of removal torque versus rotation angle behavior are plotted in Fig 9. The characteristics of the bone-implant interface failure could be qualitatively distinguished by 3 distinctive mechanical responses: (1) an initial "slip" of the interface followed by a substantial increase in torque values to a yield point and torque plateau, (2) a steadily increasing torque value until a yield point and subsequent plateau in the torque response was observed, or (3) a sharply increasing torque value terminating with a single clear failure point. All failure behaviors are characteristic of a mechanical breakdown of the osseointegrated interface. Failure mode 1 was predominantly observed with the APC surface-modified Ti implants (group 4). Failure mode 2 was characteristic of the
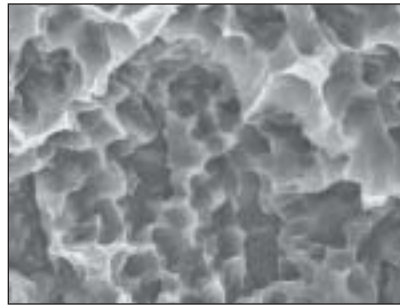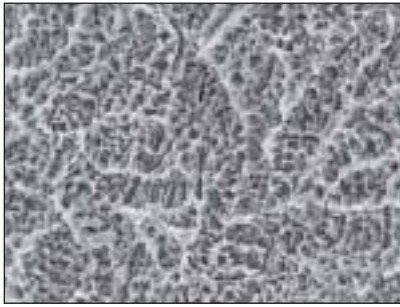
Figs 7a and 7b Scanning electron micrographs of group 5 surface (sandblasted and acid-etched titanium implant surface coated with bisphosphonate).
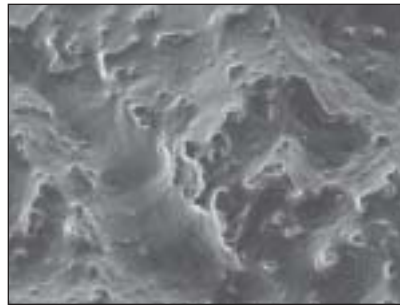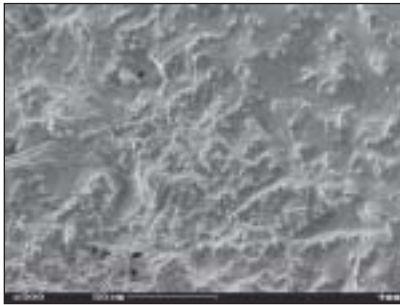
Figs 8a and 8b Scanning electron micrographs of group 6 surface (sandblasted and acid-etched titanium implant, coated with a mixture of type 1 collagen containing chondroitin sulfate).

| Table 1	Surface Topography of Each Implant Surface			
Group	S_a	S_{sk}	S_{ku}	α_w
Group 1	2.002	−0.187	2.612	1.810
Group 1	2.072	−0.113	2.535	1.815
Group 2	1.073	−0.237	2.475	1.148
Group 2	1.116	−0.273	2.700	1.151
Group 3	1.054	0.023	2.240	1.224
Group 3	1.383	−0.133	2.644	1.314
Group 4	1.415	−0.112	2.510	1.206
Group 4	1.497	−0.260	2.757	1.227
Group 5	2.239	−0.128	2.492	1.843
Group 5	2.176	−0.189	2.638	1.827
Group 6	1.702	−0.234	2.618	1.722
Group 6	1.769	−0.248	2.669	1.756

S_a = arithmetic mean deviation of the measured area; S_{sk} = skewness; S_{ku} = kurtosis; α_w = surface area ratio. Two samples of each surface were measured.

Table 2	Regional Bone Volume Density (BV/TV)					
	Bone volume density (%)					
	Week 4			**Week 8**		
Group	**Inner ring**	**Outer ring**	**% difference**	**Inner ring**	**Outer ring**	**% difference**
Group 1	28.4 ± 7.6	18.9 ± 4.7	50.2*	30.3 ± 5.1	18.6 ± 3.3	63.3***
Group 3	31.9 ± 6.2	20.4 ± 3.4	56.5**	28.5 ± 4.4	19.3 ± 4.6	47.2**
Group 4	33.8 ± 9.2	21.6 ± 3.6	56.4*	30.5 ± 4.2	21.2 ± 5.4	44.0**
Group 5	27.2 ± 7.3	17.8 ± 6.0	52.8*	32.1 ± 6.2	19.8 ± 4.6	62.0**
Group 6	29.1 ± 4.5	20.7 ± 3.0	40.6**	28.6 ± 6.8	18.5 ± 5.1	54.5*

*$P < .05$; **$P < .01$; ***$P < .001$.
Values reported are means ± SDs.
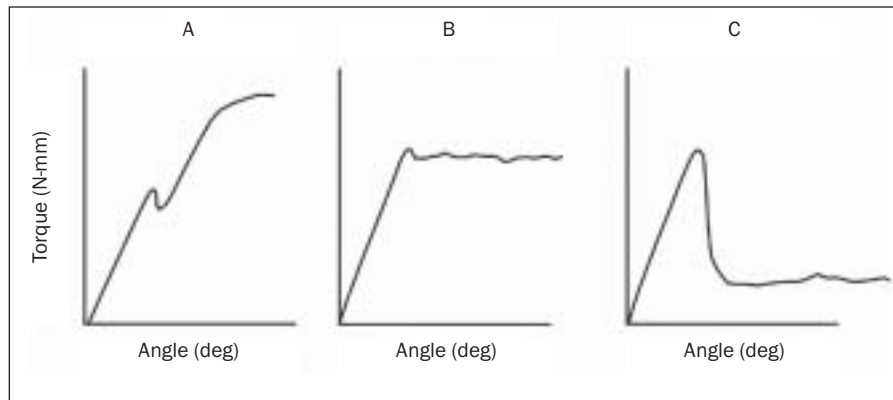
**Fig 9** Interface failure modes during biomechanical testing.

| Table 3	Removal Torque Values (Mean ± SD, in N-mm)		
Group	Week 2	Week 4	Week 8
Group 1 (Ti)	733 ± 240	1,413 ± 266	1,884 ± 227[1,2]
Group 2 (zirconia)	550 ± 112	867 ± 308	1,005 ± 281[1,3,4,5]
Group 3 (Ti + CaP)	660 ± 110	1,297 ± 166	1,683 ± 214[3,6]
Group 4 (Ti + APC)	594 ± 169	779 ± 260	919 ± 312[2,6,7,8]
Group 5 (Ti + bisphosphonate)	873 ± 196	1,438 ± 332	1,835 ± 301[4,7]
Group 6 (Ti + collagen + CS)	683 ± 115	1,462 ± 245	1,593 ± 308[5,8]

CS = chondroitin sulfate.
[4,5,6,8] $P < 0.05$;
[1,2,3,7] $P < .01$ (these numbers indicate P values for individual post-hoc comparisons between groups).
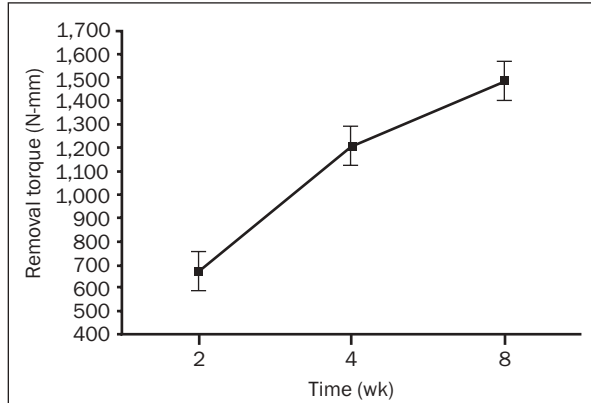
Fig 10 Time response of implant osseointegration, as determined from removal torque testing.
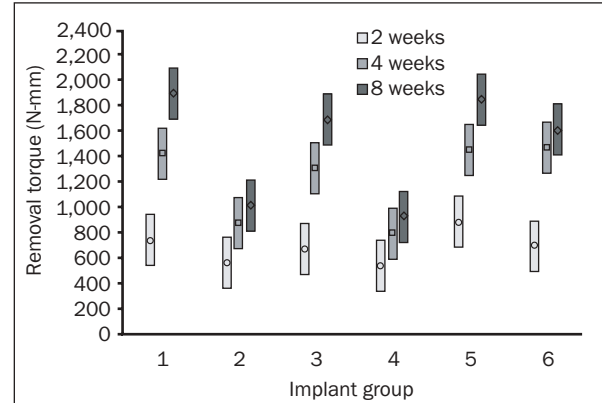

Fig 11 Interaction of implant surface type and healing period on measured removal torque values.

zirconia implants (group 2). All other implants generally demonstrated a failure of the interface corresponding to the torque curve shown in Fig 9c.

Interface removal torque values are summarized in Table 3. There was a substantial and significant increase in the removal torque values with increasing healing periods ($P < .001$; Fig 10). The implant surface was also a significant factor determining the mechanical response of the bone-implant interface ($P < .001$; Fig 11). Post hoc analysis was performed to

evaluate specific hypotheses on implant performance. After 2 weeks and 4 weeks of healing, there was no significant difference in removal torque values for any implant surface type. Specifically, apparent differences in mean removal torque values for group 5 (Ti + bisphosphonate) and group 6 (Ti + CCCS), compared to group 4, did not reach statistical significance ($P = .21$ and $P = .16$, respectively). After 8 weeks of healing, removal torque values for group 1 (Ti), group 3 (Ti + CaP), group 5 (Ti + bisphospho-
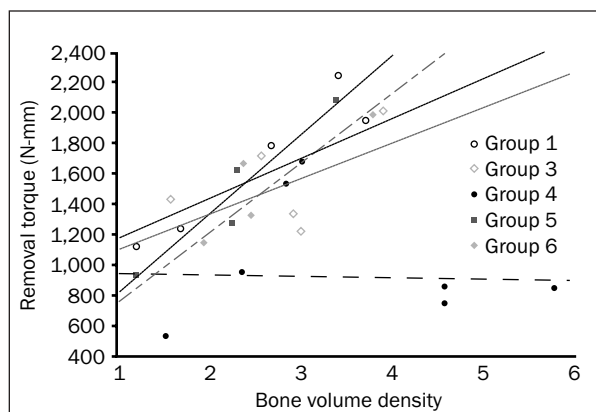
Fig 12 Correlation between local bone density and interfacial strength. Group 1 = Ti; group 3 = Ti + CaP; group 4 = Ti + APC; group 5 = Ti + bisphosphonate; group 6 = Ti + collagen containing chondroitin sulfate.

nate), and group 6 (Ti + CCCS) were significantly higher than those of group 2 (zirconia) and group 4 (Ti + APC). No statistically significant differences in removal torque values were found at 8 weeks between groups 1, 3, 5, and 6 or between groups 2 and 4. For implant group 5 (bisphosphonate) and group 6 (CCCS), a strong correlation was found between local bone density and removal torque values (r^2 = 0.92, 0.78 and P = .04, .05, respectively; Fig 12). No significant correlation was found for the other groups.

DISCUSSION

The effect of 6 different implant surface preparations on peri-implant bone healing was evaluated in vivo by comparing the biomechanical strength of the bone-implant interface, for identical implant geometries, at 3 postimplantation time points. A newly developed large animal model was used for implant evaluation, with implantation in the pelvic bone rather than in the mandible or maxilla. The principal advantage of this model is the ability to objectively compare several implant surfaces in a single animal, thereby reducing interanimal variability. Furthermore, infections caused by septic problems in the mouth did not jeopardize the overall results.

For all implant surfaces tested, there was a significant increase in interfacial strength over time. CaP, bisphosphonate, and CCCS coatings enhanced bone healing around titanium implants in comparison to titanium implants with an APC surface modification or zirconia implants with a sandblasted and etched surface. However, the biomechanical performance of these new candidate surfaces was not significantly better than that of the reference implant surface, a sandblasted, acid-etched titanium implant.

For some implant groups, a correlation between BV/TV and removal torque was found, apparently indicating that more bone leads to better implant fixation, but surface topology and bonding characteristics influenced implant fixation as well. While microCT is useful for nondestructive 3-dimensional bone ratio measurements around implants, an inherent metallic halation artifact and resolution limits potentially confound peri-implant bone assessment.[31,32] The selection of the trabecular region for analysis was based on the knowledge that remodeling proceeds faster in trabecular bone. However, significant time-dependent changes were not found in this study.

Roughened titanium surfaces are effective in enhancing the interfacial biomechanical properties of bone-anchored implants by providing a mechanical interlock.[7] Interfacial bone formation may also be promoted by roughened surfaces, as a significantly greater percentage of bone-to-implant contact has been observed adjacent to microrough titanium surfaces, in comparison to machined or polished titanium surfaces.[6,33] The results of the current study confirm the benefits of a sandblasted, acid-etched titanium implant surface, and as such this surface treatment may still be considered the gold standard. Nevertheless, it has been suggested that bioactive implants may offer some promise,[34,35] and therefore a variety of such surface modifications and coatings was evaluated in the current screening study.

Different implant coatings have been previously evaluated and shown to promote firmer bone anchorage.[36,37] CaP is a logical choice for a biomimetic coating, as the CaP-reinforced chemistry of such coatings enhances the rate of early bone formation.[38–40] However, the present study demonstrated no clear advantage for electrochemically assisted CaP-coated implants.

Zirconia implants offer esthetic benefits over titanium implants, but their mechanical potential is still being evaluated. Sennerby et al[41] reported a strong bone tissue response to surface-modified zirconia implants. In the current study, sandblasted and etched zirconia implants did not perform as well as several other candidate implant surfaces. However, zirconia and APC-treated Ti are reference implant

surfaces with good clinical results, and therefore the lower values observed should be interpreted with caution. Both APC-treated Ti and zirconia exhibited a lower surface area ratio (Table 1, Figs 4 and 6). Although the CaP group exhibited similarly low values of α_w, this was a measurement artifact caused by the restricted lateral resolution of the confocal microscope, which was confirmed by the scanning electron microscopy. The confocal microscope cannot resolve the fine crystallites of the CaP coating. The optimal surface ratio for bone growth should be around 1.5.[42] Moderate surface roughness (S_a between 1.2 and 2.0 µm) is associated with a stronger bone response than smoother or rougher surfaces.[35] Because the S_a values were also rather low for groups 2 and 4, surface topography might be one of the key factors for the low extraction torques measured at all time points. Both surfaces will have to be optimized from a topographic point of view.

Biologic enhancement of bone formation remains an elusive goal. The use of CCCS coatings to provide essential bone extracellular matrix components at the interface is a very recent development. To date, there are no reports of the mechanical performance of such implant surfaces. In the present study, a similar response was shown between bisphosphonate- and CCCS-coated implants at the 2-week and 4-week time points. Reduced torque values at week 8 for the CCCS group may indicate a remodeling process. Biochemical modification of the implant surface with CCCS has been shown to enhance new bone formation and bone-to-implant contact—potentially by the provision of binding sites for integrin receptors—and induces greater expression of bone-specific matrix proteins.[17,43–45]

The local delivery of bisphosphonates to enhance local peri-implant bone formation is a promising avenue requiring further study. A higher percentage of bone contact was found around bisphosphonate-coated implants by Yoshinari et al[46] and Peter et al.[19,47] The potentially modest increase in the early and mid-term mechanical performance of bisphosphonate-coated implants could not be statistically verified in this preliminary study. On the other hand, the strong correlation between bone density and interface mechanics observed for this implant group implies functional osseointegration, whereby stimulation of bone formation may lead to improved fixation.

Whereas removal torque values represent a valuable, objective means of appraising interfacial strength, they do not fully and uniquely characterize the process of bone healing. Histomorphometric analyses are underway and will provide a more complete evaluation of the potential for such functional surface modifications to influence the rate and amount of bone-implant contact.

CONCLUSIONS

A variety of surface modifications for dental implants were evaluated in an in vivo study, with mechanical testing of the bone-implant interface strength and nondestructive evaluation of bone quality by microCT. The results of the mechanical testing indicate that coatings of calcium phosphate, bisphosphonate, and collagen containing chondroitin sulfate all have the potential to enhance peri-implant bone healing, but a significant difference from the performance of the reference standard of a sandblasted, acid-etched titanium implant could not be shown.

ACKNOWLEDGMENTS

REFERENCES

1. Albrektsson T, Brånemark P-I, Hansson HA, Lindstrom J. Osseointegrated titanium implants. Requirements for ensuring a long-lasting, direct bone-to-implant anchorage in man. Acta Orthop Scand 1981;52:155–170.
2. Ratner BD, Porter SC. Surfaces in biology and biomaterials; description and characterization. In: Brash JLW (ed). Interfacial Phenomena and Bioproducts. New York: Marcel Dekker, 1996:57–83.
3. Wieland M, Sittig C, Brunette DM, Textor M, Spencer ND. Measurement and evaluation of the chemical composition and topography of titanium implant surfaces. In: Davies JE (ed). Bone Engineering. Toronto: ed squared inc, 2000:163–182.
4. Buser D, Schenk RK, Steinemann S, Fiorellini JP, Fox CH, Stich H. Influence of surface characteristics on bone integration of titanium implants. A histomorphometric study in miniature pigs. J Biomed Mater Res 1991;25:889–902.
5. Cochran DL, Schenk RK, Lussi A, Higginbottom FL, Buser D. Bone response to unloaded and loaded titanium implants with a sandblasted and acid-etched surface: A histometric study in the canine mandible. J Biomed Mater Res 1998;40:1–11.
6. Buser D, Nydegger T, Oxland T, et al. Interface shear strength of titanium implants with a sandblasted and acid-etched surface: A biomechanical study in the maxilla of miniature pigs. J Biomed Mater Res 1999;45:75–83.
7. Li D, Ferguson SJ, Beutler T, et al. Biomechanical comparison of the sandblasted and acid-etched and the machined and acid-etched titanium surface for dental implants. J Biomed Mater Res 2002;60:325–332.
8. Roccuzzo M, Bunino M, Prioglio F, Bianchi SD. Early loading of sandblasted and acid-etched (SLA) implants: A prospective split-mouth comparative study. Clin Oral Implants Res 2001;12:572–578.
9. Cochran DL, Buser D, ten Bruggenkate CM, et al. The use of reduced healing times on ITI implants with a sandblasted and acid-etched (SLA) surface: Early results from clinical trials on ITI SLA implants. Clin Oral Implants Res 2002;13:144–153.

10. Bornstein MM, Schmid B, Belser UC, Lussi A, Buser D. Early loading of non-submerged titanium implants with a sandblasted and acid-etched (SLA) surface: 5-year results of a prospective study in partially edentulous patients. Clin Oral Implants Res 2005;16:631–638.

11. Bornstein MM, Lussi A, Schmid B, Belser UC, Buser D. Early loading of nonsubmerged titanium implants with a sandblasted and acid-etched (SLA) surface: 3-year results of a prospective study in partially edentulous patients. Int J Oral Maxillofac Implants 2003;18:659–666.

12. Ferguson SJ, Broggini N, Wieland M, et al. Biomechanical evaluation of the interfacial strength of a chemically modified sandblasted and acid-etched titanium surface. J Biomed Mater Res A 2006;78:291–297.

13. Schliephake H, Scharnweber D, Roesseler S, Dard M, Sewing A, Aref A. Biomimetic calcium phosphate composite coating of dental implants. Int J Oral Maxillofac Implants 2006;21:738–746.

14. Barrere F, Layrolle P, Van Blitterswijk CA, De Groot K. Biomimetic coatings on titanium: A crystal growth study of octacalcium phosphate. J Mater Sci Mater Med 2001;12:529–534.

15. Cooper LF, Zhou Y, Takebe J, et al. Fluoride modification effects on osteoblast behavior and bone formation at TiO_2 grit-blasted c.p. titanium endosseous implants. Biomaterials 2006;27:926–936.

16. Schuler M, Owen GR, Hamilton DW, et al. Biomimetic modification of titanium dental implant model surfaces using the RGDSP-peptide sequence: A cell morphology study. Biomaterials 2006; 27:4003–4015.

17. Rammelt S, Illert T, Bierbaum S, Scharnweber D, Zwipp H, Schneiders W. Coating of titanium implants with collagen, RGD peptide and chondroitin sulfate. Biomaterials 2006;27:5561–5571.

18. Michael J, Beutner R, Hempel U, Scharnweber D, Worch H, Schwenzer B. Surface modification of titanium-based alloys with bioactive molecules using electrochemically fixed nucleic acids. J Biomed Mater Res B Appl Biomater 2007;80:146–155.

19. Peter B, Gauthier O, Laib S, et al. Local delivery of bisphosphonate from coated orthopedic implants increases implants mechanical stability in osteoporotic rats. J Biomed Mater Res A 2006;76:133–143.

20. Fiorellini JP, Buser D, Riley E, Howell TH. Effect on bone healing of bone morphogenetic protein placed in combination with endosseous implants: A pilot study in beagle dogs. Int J Periodontics Restorative Dent 2001;21:41–47.

21. Jones AA, Buser D, Schenk R, Wozney J, Cochran DL. The effect of rhBMP-2 around endosseous implants with and without membranes in the canine model. J Periodontol 2006;77:1184–1193.

22. Becker P, Neumann HG, Nebe B, Luthen F, Rychly J. Cellular investigations on electrochemically deposited calcium phosphate composites. J Mater Sci Mater Med 2004;15(4):437–440.

23. Frauchiger VM, Schlottig F, Gasser B, Textor M. Anodic plasma-chemical treatment of CP titanium surfaces for biomedical applications. Biomaterials 2004;25:593–606.

24. Bierbaum S, Douglas T, Hanke T, et al. Collageneous matrix coatings on titanium implants modified with decorin and chondroitin sulfate: Characterization and influence on osteoblastic cells. J Biomed Mater Res A 2006;77:551–562.

25. Aerssens J, Boonen S, Lowet G, Dequeker J. Interspecies differences in bone composition, density, and quality: Potential implications for in vivo bone research. Endocrinology 1998;139:663–670.

26. Nunamaker DM, Perren SM. A radiological and histological analysis of fracture healing using prebending of compression plates. Clin Orthop Relat Res 1979;167–174.

27. Lekholm U, Zarb GA, Albrektsson T. Patient selection and preparation. In: Brånemark P-I, Zarb GA, Albrektsson T (eds). Tissue-Integrated Prostheses. Chicago: Quintessence, 1985:199–209.

28. Ruegsegger P, Koller B, Muller R. A microtomographic system for the nondestructive evaluation of bone architecture. Calcif Tissue Int 1996;58:24–29.

29. van Lenthe GH, Hagenmuller H, Bohner M, Hollister SJ, Meinel L, Muller R. Nondestructive micro-computed tomography for biological imaging and quantification of scaffold-bone interaction in vivo. Biomaterials 2007; 28:2479–2490.

30. Müller R, Hildebrand T, Häuselmann HJ, Rüegsegger P. In vivo reproducibility of three-dimensional structural properties of noninvasive bone biopsies using 3D-pQCT. J Bone Miner Res 1996;11(11):1745–1750.

31. Butz F, Ogawa T, Chang TL, Nishimura I. Three-dimensional bone-implant integration profiling using micro-computed tomography. Int J Oral Maxillofac Implants 2006;21:687–695.

32. Van Oosterwyck H, Duyck J, Vander Sloten J, et al. Use of micro-focus computerized tomography as a new technique for characterizing bone tissue around oral implants. J Oral Implantol 2000;26:5–12.

33. Wennerberg A, Albrektsson T, Andersson B, Krol JJ. A histomorphometric and removal torque study of screw-shaped titanium implants with three different surface topographies. Clin Oral Implants Res 1995;6:24–30.

34. Albrektsson T, Wennerberg A. Oral implant surfaces: Part 2—Review focusing on clinical knowledge of different surfaces. Int J Prosthodont 2004;17:544–564.

35. Albrektsson T, Wennerberg A. Oral implant surfaces: Part 1—Review focusing on topographic and chemical properties of different surfaces and in vivo responses to them. Int J Prosthodont 2004;17:536–543.

36. Ellingsen JE, Johansson CB, Wennerberg A, Holmen A. Improved retention and bone-tolmplant contact with fluoride-modified titanium implants. Int J Oral Maxillofac Implants 2004;19:659–666.

37. Giavaresi G, Branda F, Causa F, et al. Poly(2-hydroxyethyl methacrylate) biomimetic coating to improve osseointegration of a PMMA/HA/glass composite implant: In vivo mechanical and histomorphometric assessments. Int J Artif Organs 2004;27:674–680.

38. Sul YT, Byon ES, Jeong Y. Biomechanical measurements of calcium-incorporated oxidized implants in rabbit bone: Effect of calcium surface chemistry of a novel implant. Clin Implant Dent Relat Res 2004;6:101–110.

39. Gan L, Wang J, Tache A, Valiquette N, Deporter D, Pilliar R. Calcium phosphate sol-gel-derived thin films on porous-surfaced implants for enhanced osteoconductivity. Part II: Short-term in vivo studies. Biomaterials 2004;25:5313–5321.

40. Tache A, Gan L, Deporter D, Pilliar RM. Effect of surface chemistry on the rate of osseointegration of sintered porous-surfaced Ti-6Al-4V implants. Int J Oral Maxillofac Implants 2004;19:19–29.

41. Sennerby L, Dasmah A, Larsson B, Iverhed M. Bone tissue responses to surface-modified zirconia implants: A histomorphometric and removal torque study in the rabbit. Clin Implant Dent Relat Res 2005;7(suppl 1):S13–20.

42. Wennerberg A. On Surface Roughness and Implant Incorporation [thesis]. Göteborg: Göteborg University, 1996.

43. Rammelt S, Schulze E, Bernhardt R, et al. Coating of titanium implants with type-I collagen. J Orthop Res 2004;22:1025–1034.

44. Morra M, Cassinelli C, Cascardo G, et al. Collagen I-coated titanium surfaces: Mesenchymal cell adhesion and in vivo evaluation in trabecular bone implants. J Biomed Mater Res A 2006;78: 449–458.

45. Morra M, Cassinelli C, Cascardo G, et al. Surface engineering of titanium by collagen immobilization. Surface characterization and in vitro and in vivo studies. Biomaterials 2003;24:4639–4654.

46. Yoshinari M, Oda Y, Inoue T, Matsuzaka K, Shimono M. Bone response to calcium phosphate-coated and bisphosphonate-immobilized titanium implants. Biomaterials 2002;23:2879–2885.

47. Peter B, Pioletti DP, Laib S, et al. Calcium phosphate drug delivery system: Influence of local zoledronate release on bone implant osseointegration. Bone 2005;36:52–60.